A dissociated dislocation in an ultra thin silicon plate

Sami Youssef, Roland Bonnet

A dissociated dislocation in an ultra thin silicon plate

Journal:	*Philosophical Magazine & Philosophical Magazine Letters*
Manuscript ID:	TPHM-05-Dec-0571.R1
Journal Selection:	Philosophical Magazine
Date Submitted by the Author:	02-Mar-2006
Complete List of Authors:	Youssef, Sami; Faculté des Sciences de Monastir, Unité de Recherche Physique des Solides BONNET, Roland; CNRS
Keywords:	thin-film silicon, dislocation theory, nanomechanics
Keywords (user supplied):	thin plate

A dissociated dislocation in an ultra thin silicon plate

SAMI YOUSSEF † and ROLAND BONNET † †

† Unité de Recherche Physique des Solides, Faculté des Sciences de Monastir, Avenue de l'Environnement, 5019, Monastir, Tunisie

† † Institut National Polytechnique de Grenoble (LTPCM/ENSEEG, CNRS UMR 5614), D. U., BP 75, 38402 Saint Martin d'Hères, France

Simplified explicit expressions are firstly presented to describe the elastic displacement field of a periodic family of misfit dislocations running parallel to the two free surfaces of an elastically isotropic plate. In the situation where the period tends to infinity, the use of these expressions proves to be quite valuable to investigate the change of the separation distance S between two partial dislocations as a function of the position of one partial and orientation of the fault plane. For the two 30° Shockley partials of a dissociated screw dislocation in an ultra thin silicon plate, numerical results indicate that S can change drastically. This property is confirmed in anisotropic elasticity for a dislocation located nearby the free surface of a semi infinite crystal. These results emphasize that a particular attention should be paid to precise measurements of the local thickness and positions of the partials when weak beam or high resolution experiments in transmission electron microscopy are used.

Keywords : thin plate, silicon, free surfaces, dislocation, elasticity

1. Introduction

The use of thinner and thinner plates to investigate the fine structures of materials by high resolution transmission electron microscopy (HRTEM) puts new questions relative to free surface effects due to the confinement of dislocations in the plate. Here, the authors report on a description of the elastic displacement field of a dislocation of any Burgers vector **b** with the aid of a two-dimensional theory leading to fully explicit expressions. In the past, the stress field of a dislocation of direction **U** running parallel to the boundary was found by three different authors : Leibfried and Dietze [1] for the screw component, then Kroupa [2] for the edge component parallel to the plate surfaces, and finally Lee and Dundurs [3] for the edge component parallel to the normal **N** to the surfaces (see Appendix 1). One of the present authors also solved this problem from two other different approaches, the interest of which is to provide the full elastic field (stresses and displacement **u**). One is based on a Fourier series solution [4] and applies to a periodic family of misfit dislocations at the interface of a heterophase bicrystal and the other is expressed from the solution of a system of two integral equations [5]. However, the numerical convergence of all these solutions is not as rapid as one would wish for applications. The Fourier series is slowly converging close to the dislocation line (Gibbs phenomenon), while the solutions in [2,3,5] involve integration quadratures and, for the dummy variable of integration, inaccessible limits at zero and infinite.

In the first part of the present work, it is shown that, for an elastically isotropic plate, the expressions of **u** derived in [4] can be greatly simplified so as to obtain short and explicit formulae and therefore a much better numerical efficiency. In addition to providing these simplified expressions, the present study investigates the change of the separation distance S between two partials of a dissociated dislocation in silicon (parameter a= 0.54282 nm [6]). Since the first observations of the separation of perfect dislocations [7,8], dislocations in silicon have been investigated in numerous works by weak-beam microscopy and HRTEM, e. g., [9-18]. In particular, the intrinsic mobility and the possible atomic structures of the (near) screw dislocations with Burgers vector 1/2<110> are topics of intense activity, see, e. g., [19-22]. When some thermo-mechanical conditions are fulfilled, the screw dislocation appear to dissociate into two 30° Shockley partials moving on the so-called "glide" or "shuffle" set [23]. In particular, Cai et al. [20]

Corresponding author. Email : rbonnet@ltpcm.inpg.fr

have shown that its mobility depends strongly on the spacing S separating the partials, which stresses the importance to measure precisely this parameter. Most measurements of S were performed from weak-beam TEM observations on screw dislocations running in a direction <110> roughly parallel to the average plane of the thin plate. They often lie either on a {111} gliding plane [9-12] or a {001} low-angle twist boundary [17,18,24,25]. Plan view images taken under HRTEM conditions were also used [16] in the hope to visualize possible kinks along the partials, the plate thickness being extremely small, about 4 nm. On the other hand, previous measurements of the separation distance S of the dissociated screw dislocation reveals a large spread in the values since it lies in the range 2.3 nm [24] to 5.8 nm [11]. High internal stresses can doubtless contribute to the cause of this large spread of S, among which free surface effects very difficult to handle on a rigorous basis, despite some qualitative or quantitative observations of elastic relaxation due to these surfaces, e. g., [26-30]. It will be shown in §3 that S can depend drastically, in an ultra thin plate, on the position and orientation of the fault plane.

§2. DISLOCATIONS IN AN ISOTROPIC THIN PLATE

As outlined above, the theoretical approach starts from the knowledge of the displacement field **u** of a family of undissociated, infinitely long, misfit dislocations [4], periodically distributed along the interface of a thin bicrystal with the period Λ, figure 1. The boundary conditions in stresses and displacements along the interface are those taken in [31], while at the two free surfaces the external applied forces are zero.

For the sake of clarity, symbols and conventions are now presented. Figure 1 represents the Cartesian frame $Ox_1x_2x_3$ attached to one of these dislocations for which Ox_3 // **U**. Its Burgers vector is **b** with components (b_1,b_2,b_3). The normal to the plate is accordingly **N** // Ox_2. The interface separates two crystals denoted + and – according to their positions with respect to $x_2 > 0$ or $x_2 < 0$. Their thicknesses are respectively h^+ and h^-, while that of the bicrystal is consequently $h = h^+ + h^-$.

If Λ tends to infinity the misfit between the two crystals tends to zero and the elastic field around the dislocation lying along Ox_3 tends asymptotically towards that of a translation dislocation [23, 32]. Since the shear modulus μ and the Poisson ratio ν of the two crystals are identical, closed form formulae can be obtained from [4]. Its **u** field can be written, for each crystal, as

$$u_k = \sum_{\substack{-\infty \\ n\neq 0}}^{\infty} U_k^{(n)} e^{i\,n\,\omega\,x_1} \qquad (1)$$

expression in which $\omega = 2\pi/\Lambda$ and

$$U_1^{(n)} = (P + Q\,n\,\omega\,x_2)e^{-n\,\omega\,x_2} + (R + S\,n\,\omega\,x_2)e^{n\,\omega\,x_2} \qquad (2)$$

$$U_2^{(n)} = i\left[(P + Q(3-4\nu) + Q\,n\,\omega\,x_2)\right]e^{-n\,\omega\,x_2} - i\left[(R - S(3-4\nu) + S\,n\,\omega\,x_2)\right]e^{n\,\omega\,x_2} \qquad (3)$$

$$U_3^{(n)} = T\,e^{-n\,\omega\,x_2} + V\,e^{n\,\omega\,x_2} \qquad (4)$$

The simplified expressions of the complex constants P, Q, R, S, T, V written in [4] have been derived after corrections of some minor typographical errors (see Appendix 1). For the general term of order n they are the following

$$P^+ = \frac{2\,i\,b_1\,(-1+\nu) + b_2(1-2\nu)}{8\,\pi\,n\,(-1+\nu)} + P^-, \qquad (6)$$

$$Q^+ = \frac{i\,b_1 - b_2}{8\,\pi\,n\,(-1+\nu)} + Q^-, \qquad (7)$$

Corresponding author. Email : rbonnet@ltpcm.inpg.fr

$$R^+ = \frac{2\,i\,b_1(1-\nu)+\,b_2(1-2\nu)}{8\,\pi\,n\,(1-\nu)} + (\,P^-(\,3-4\nu+2\,n\,\omega\,h^-\,)+ \qquad (8)$$

$$2\,Q^-(\,2-6\nu+4\,\nu^2-n^2\,\omega^2\,(h^-)^2\,))\,e^{2\,h^-\,n\,\omega}$$

$$S^+ = \frac{i\,b_1+\,b_2}{8\,\pi\,n\,(1-\nu)} + (\,2P^- + Q^-(\,3-4\nu-2\,n\quad\omega\quad h^-\,))\,e^{2\,h^-\,n\,\omega}, \qquad (9)$$

$$R^- = R^+ - \frac{2\,i\,b_1(1-\nu)+\,b_2(1-2\nu)}{8\,\pi\,n\,(1-\nu)}, \qquad (10)$$

$$S^- = S^+ - \frac{i\,b_1+\,b_2}{8\,\pi n\,(1-\nu)}, \qquad (11)$$

$$Q^- = \left\{\begin{array}{l} b_2(-1-e^{2(h+h^+)n\omega}(1+2\,h^-n\,\omega)+e^{2\,h^+n\,\omega}(1-2\;h^+n\,\omega)+ \\ e^{2\,h\,n\,\omega}(1+2\,h\,n\,\omega(1+2\;h^+n\,\omega)))-i\,b_1(-1+e^{2\,h^+n\,\omega}(1+2\,h^+n\,\omega)+ \\ e^{2\,h^-n\,\omega}(1+e^{2\,h^+n\,\omega}(-1+2\,h^-n\,\omega)+2\,h\,n\,\omega(-1+2\;h^+n\,\omega)))) \end{array}\right\}/\,\Delta\,, \qquad 12)$$

$$P^- = \left\{\begin{array}{l} 2\,i\,b_1(-1+\nu+e^{2(h+h^+)\,n\,\omega}(\,\nu-2\nu\,h^-n\,\omega-(1-h^-n\,\omega)^2\,)+ \\ e^{2\,h^+\,n\,\omega}((1+h^+n\,\omega)^2\,-\nu(1+2\,h^+n\,\omega))+e^{2\,h\,n\,\omega}(1+\nu\,(-1+2\;h\,n\,\omega\,(1-2\,h^+n\,\omega))- \\ h\,n\,\omega(2+n\,\omega\,(-h^-\,-3\,h^+\,+2\,h^+h^-n\,\omega)\,)))+b_2(1-2\nu+e^{2(h+h^+)\,n\,\omega}(1-2\,h^-n\,\omega \\ (-1+h^-n\,\omega)-2\nu(1+2\,h^-\,n\,\omega))+e^{2\,h^+\,n\,\omega}(-1+\nu\,(2-4\,h^+n\,\omega)+2\,h^+n\,\omega\,(1+h^+n\,\omega)\,)+ \\ e^{2\,h\,n\,\omega}(-1+2\nu\,(1+2\;h\,n\,\omega\,(1+2\,h^+n\,\omega))+2\,h\,n\,\omega(-1+n\,\omega\,(h^-\,-3\,h^+\,+2\,h^+h^-n\,\omega)\,))) \end{array}\right\}/\,\Delta \qquad (13)$$

$$\Delta = 8\,\pi\,n\,(-1+\nu)\,(-1-e^{4\,h\,n\,\omega}+e^{2\,h\,n\,\omega}(2+4\,h^2n^2\,\omega^2\,)), \qquad (14)$$

$$T^+ = i\,b_3\,e^{2\,h^+\,n\,\omega}(-1+e^{2\,h^-\,n\,\omega}\,)(-1+Coth(h\,n\,\omega))/(8\,\pi\,n\,), \qquad (15)$$

$$V^+ = i\,b_3\,(-1+e^{2\,h^-\,n\,\omega}\,)(-1+Coth(h\,n\,\omega))/(8\,\pi\,n\,), \qquad (16)$$

$$T^- = -\,i\,b_3\,(-1+e^{2\,h^+\,n\,\omega}\,)(-1+Coth(h\,n\,\omega))/(8\,\pi\,n\,), \qquad (17)$$

$$V^- = -\,i\,b_3\,e^{2\,h^-\,n\,\omega}(-1+e^{2\,h^+\,n\,\omega}\,)(-1+Coth(h\,n\,\omega))/(8\,\pi\,n\,). \qquad (18)$$

Application of the Hooke law and extraction of real part then permits derivation of the stress tensor σ_{ij} from Eq. (1).

To improve the slow numerical convergence of the Fourier series nearby the dislocation lines, due to the Gibbs phenomenon of discontinuous series, the Fourier harmonics of large order can be reduced to their principal terms, i. e. those for which n > N, N being an integer sufficiently large. The analytic forms of these principal terms are sufficiently simple for them to be summed exactly when n goes to infinity, thanks to analytical well-known functions [33].

§3. DEPENDENCE OF THE DISLOCATION SPACING ON THE FAULT PLANE ORIENTATION

3.1 The mechanical equilibrium

Let us suppose that two partial dislocations 1 and 2, running parallel to the two free surfaces of the plate, are linked by a fault plane with the fault energy per unit surface γ. Their separation distance S can be determined from mechanical equilibrium. Dislocation 1 has the Burgers vector $\mathbf{b}^{(1)}$, is supposed fixed along Ox_3 in figure 1, and is oriented by this axis. When the crystallographic direction of the normal **N** to the plate changes, the normal **n** to the fault plane turns around Ox_3 with the polar angle α= (**N**,**n**), and drags dislocation 2 with Burgers vector $\mathbf{b}^{(2)}$. The separation distance

Corresponding author. Email : rbonnet@ltpcm.inpg.fr

S is therefore changing with α because of the elastic relaxation effect. A small virtual displacement dS of dislocation 2 along the fault plane will work in the stress field $\sigma_{ij}^{(1)}$ generated by dislocation 1 and produce the following small energy change per unit length (with the usual summation convention)

$$dW = (\gamma - \sigma_{ij}^{(1)} n_j b_i^{(2)})dS \,. \qquad (19)$$

The equilibrium is reached when the second member of this equation is zero.

Since the question here is to treat the equilibrium of an isolated screw dislocation, the stress field $\sigma_{ij}^{(1)}$ must be that of misfit dislocations extremely distant from each other to approach asymptotically that of a translation dislocation when the period Λ tends to infinity.

3.2 Application to the dissociated screw dislocation in silicon. Data.

In this section, Eq. (19) is applied to determine the equilibrium of the dissociated screw dislocation in silicon. The fault plane is assumed to be of intrinsic type. Partials 1 and 2 have the Burgers $\mathbf{b}^{(1)} = 1/6[\bar{1}\ 1\ 2]$ and $\mathbf{b}^{(2)} = 1/6[1\ 2\ 1]$.

For our application to ultra thin plates, the geometries are the following : Λ = 100 h with h = 4 to 20 nm. For the summation of the Fourier series, the value N= 350 was retained because larger N values do not produce any sensitive effect on the graphs of the stress field around a dislocation line. With these values, it has been verified that graphs representing various stress fields around Ox_3 are not discernible (by eye) from other graphs derived from application of expressions given in ref. [1-3] (see Appendix 1).

The isotropic elastic constants μ and ν taken for silicon were evaluated from the anisotropic constants C_{ij} given in [23], en GPa, C_{11}=165.7, C_{12}= 63.9, C_{44}= 79.6, and a procedure proposed in [34] to average the elastic behaviour of an anisotropic crystal submitted to virtual tensile tests in all spatial directions. The results are μ = 66.11 GPa and ν = 0.229. In passing, the elastic anisotropy of silicon is small since its anisotropy factor is $2\,C_{44}/(C_{11}-C_{12}) = 1.56$.

The adopted value γ of the intrinsic fault energy needs a brief comment. For the infinite silicon crystal, a mean separation of 4.0 nm was measured in [12,13], values very close to those given in [8,20], i. e., respectively 4.1 nm and $10\ a/\sqrt{2} = 3.84$ nm. Using elastic anisotropy and a separation distance of 4 nm, the solution of a relation similar to (19) gives γ= 51.39 mJ/m2, the value adopted in the present work. With this fault energy, the application of relation (19) to an infinite isotropic medium requires a separation distance S^{∞}= 4.28 nm, slightly different from the mean separation of 4.0 nm. Note in passing that, from the isotropic elastic constants given in [23], a larger value 4.46 nm is obtained.

On the other hand, to avoid numerical difficulties due to products of exponential functions with very large and opposite exponents, the calculation programme is built to include digits of precision equal to 32 in the numbers [33]. With our desk computer, and for the smaller thicknesses h investigated, a consuming time of a few minutes is enough to draw a curve exhibiting the locus of partial 2 for all orientations of the fault plane.

To obtain a better insight on the independent effect of each surface on the locus of partial 2, calculations have been performed with h^+ much larger than h^-. In this case, the elastic field tends to that of a straight dislocation located parallel and close to the bottom free surface of a semi-infinite substrate, see [23] for the screw component and [35,36] for the two edge components (see also Appendix 1). The quasi-identity of the graphs corresponding to a dislocation located in a bottom-limited semi-infinite crystal and in a thin plate with h^+= 25 nm and h^- = 5 nm were verified numerically. The converse situation of a top-limited semi-infinite substrate (h^- tends to infinity) and a plate with h^+= 5 nm and h^- = 25 nm was also verified.

Corresponding author. Email : rbonnet@ltpcm.inpg.fr

§4. RESULTS AND DISCUSSION

Free surface relaxation effects of the dissociated [0 1 1] screw dislocation are investigated for five isotropic silicon plates (thicknesses h=4 to 20 nm) and illustrated in figures 2(a-e). The plain curve of each graph describes the change of the separation distance S when partial 1 is fixed in the median plane of the plate and partial 2 is turning around partial 1. In figure 2(d), **n** is the fault normal and the distance 1-2 in dotted lines represents the equilibrium distance S between partials 1 and 2 for a given polar angle α. The plain curves are consequently the locus of partial 2 when α is changing. The case of an infinite silicon crystal is quite different since this locus is simply the circle in dotted lines (radius S^{∞}= 4.28 nm).

Since isotropy is assumed, the locus of partial 2 exhibits symmetry with respect to the axes Ox_1 and Ox_2. The equilibrium calculation can therefore be limited inside the interval $0 < \alpha < 90°$. Three types of configurations are possible:

- If h < 15 nm (approximately), the locus of partial 2 in the plate describes a vertical barrel-shape profile. Therefore, partial 2 cannot find any equilibrium in the plate if the fault plane is too largely inclined with respect to Ox_1. In figures 2(a-c), h= 4, 8 and 12 nm, stability is only possible for $|\alpha| < 45°$, 55° and 63° respectively. In figure 2(a), h = 4 nm and α = 0, the separation distance falls down to 3.08 nm. The contraction of S is 27.9% with respect to S^{∞}. For h= 3 nm and α = 0, i. e., a situation very close to that taken in the experimental work by HRTEM of Suzuki et al. [16], S= 2.6 nm (39% contraction).

- If 15 nm < h < 17.8 nm, e. g. figure 2(d), the locus of partial 2 looks like a symmetric egg-cup with two symmetrical necks nearby the free surfaces. For h approaching 17.8 nm, the necks become narrower and narrower until they transform in points.

- If h > 17.8 nm, e. g. figure 2(e), the locus of partial 2 is complex since three disconnected curves are possible according to the value of α. In this figure, three possible dissociations 1-2 are represented. A closed curve surrounds the central circle in dotted line (infinite case), while two circular segments are placed near the two free surfaces. Therefore, a fault plane oriented with an angle $|\alpha|$ close to 90° give rise to two possible equilibriums.

- For larger and larger h, the central curve tends gradually to the circle in dotted line while the circular-shape segments nearby the free surfaces have lengths tending to 0.

For an easier comparison of the independent effect of the two free surfaces on the separation S, the case of a bottom-limited semi-infinite crystal is also considered in figures 3(a-e). The distance $\bar{h}$ between partial 1 and the bottom free surface takes the same values as for the plate in figures 2(a-e). The geometrical forms of the loci of partial 2 for $x_2 < 0$, in figures 2(a-e) and 3(a-e), look at first sight similar. A unique plain curve describes the locus of partial 2 for $\bar{h} < 11.45$ nm, against $\bar{h} <$ 8.8 nm for a plate. These critical values of $\bar{h}$ give an idea of the intensity of the relaxation phenomena, much stronger for the plate.

In view of the variety of the equilibrium curves depicted in figures 2(a-e) and 3(a-e), a further investigation was undertaken to determine if any unstable mechanical balance can be present. To simplify, calculations were only performed for a semi-infinite crystal and a thickness range including a necking phenomenon in the locus of partial 2. Besides, despite the small anisotropy ratio of silicon, anisotropic elasticity was also applied to calculate the locus of partial 2. The corresponding elastic field is that already tested in [37], see also Appendix 1. Of course, for these latter calculations, the elastic constants relative to $Ox_1x_2x_3$ change with α. From Eq. (19), numerical maps of the second derivatives d^2W/dS^2 were calculated for each case, using:

- isotropy and $\bar{h}$= 10, 11 and 11.5 nm (very close to zero necking), figures 4(a-c),
- anisotropy and $\bar{h}$= 10, 10.5 (very close to zero necking), and 11.5 nm, figures (d-f).

Corresponding author. Email : rbonnet@ltpcm.inpg.fr

In these figures, the thicker bottom curves are obtained for $d^2W/dS^2 = 0$. They separate regions where stability ($d^2W/dS^2 > 0$) or instability ($d^2W/dS^2 < 0$, shaded regions) of the mechanical equilibrium occurs for partial 2.

In isotropy, partial 2 is stable in figure 4(a) for any **n**, except those orientations for which the polar radius 1-2 cuts the bottom free surface. An extreme separation distance equal to about 2.5 S^∞ for $\alpha = -70°$ is therefore predicted for a partial 2 very close to the free surface, a case for which the elastic field of partial 2 would vanish. For figures 4(b,c), the equilibriums corresponding to partial 2 along the plain curves and inside the shaded regions are unstable. In figure 4(c), two possible dissociation planes 1-2 are depicted in dotted lines, one is stable (shorter distance S) and the other is unstable (larger distance S).

For the infinite anisotropic silicon, the circles in dotted lines in figures 4(d-f) correspond to $S^\infty = 4.0$ nm, the measured values in [12, 13].

For the semi-infinite anisotropic silicon, the graphs in figures 4(d-f) are roughly similar to figures 4(a-c). For each graph, a slight asymmetric behaviour of the dissociation is visible with respect to the vertical plane $x_1 = 0$, also visible in the limiting curves of the shaded regions associated to instability. In figures 4(d,e), on the left hand side, very small branches of the plain curves are outside the shaded region and could give rise to a stable partial 2 very close to the free surface. In figure 4(f), stability is always obtained with a partial 2 on the closed loop of plain curve, while instability is predicted for a partial 2 located on the plain curve inside the shaded region. Anisotropy influences slightly the zero necking phenomenon for the semi-infinite silicon ($h^- = 10.6$ nm in anisotropy against 11.45 nm in isotropy).

§5. CONCLUSION

The displacement field **u** of a straight translation dislocation lying parallel to the two free surfaces of an ultra thin isotropic plate can be found as the limit of a solution valid for a periodic family of misfit dislocations. Its interest is to provide an explicit and simple solution for **u**, contrary to the way followed in previous works where integration quadratures with a dummy variable tending to zero or infinity are required. It is potentially able to treat a number of partial dislocations greater than two, coplanar or not, with any Burgers vector.

An illustration of this solution to a dissociated [011] screw dislocation in silicon shows that the distance S separating the two 30° Shockley partials depends largely on the geometry of the dissociation in the plate. For the calculation, one partial (partial 1) is fixed in the middle of the plate and the other (partial 2) is positioned around partial 1 by the orientation of the fault plane and mechanical equilibrium.

For $h < 5$ nm, which is of use in high resolution TEM for silicon [16], and a fault plane almost parallel to the median plane of the plate, the distance S is much lower than in an infinite medium, by about 20 or 30%. Such a situation can be met in high resolution TEM, see e. g. [16]. If the fault plane is inclined by angles greater than about 45° with respect to the median plane, partial 2 can escape from the plate by glide because of strong image forces associated to free surfaces.

For $5 \text{ nm} < h < 17.6$ nm, the locus of partial 2 resembles successively a barrel-shape profile ($h < 15$ nm) and an egg-cup ($15 \text{ nm} < h < 18$ nm).

For $h > 17.6$ nm, the locus is described by three disconnected curves, the central one being very close to a circle describing the locus of partials 2 for an infinite crystal.

It has been shown that instability of the mechanical equilibrium may occur for $h > 17.6$ nm and inclined fault planes with a Shockley partial located nearby one free surface.

The anisotropic elasticity of silicon, only taken into account for a dissociated dislocation nearby a free surface of silicon, is proved to be of small impact on the mechanical instability of the dissociation, although some asymmetry properties arise in the separation distance between the two partials.

Corresponding author. Email : rbonnet@ltpcm.inpg.fr

It is noteworthy that such thickness scales and inclined {111} planes are commonly encountered in TEM investigations in silicon, the interface normal being close to <001> or <111>, see [8-18]. It is also expected that the relaxation phenomena described in the present work should be amplified for materials with much lower γ fault energies than that of silicon. Dissociated dislocations with edge character should also interact more strongly with the free surfaces of the plate.

Finally, it has been shown in the present work that the influence of foil thickness and dislocation depth in a thin foil can contributes severely to a systematic uncertainty in the measurement by TEM of the separation distance between two partials. This fact, already stressed years ago in [38], remains to clarify for highly anisotropic plates, a work in progress.

Acknowledgments

The authors would like to thank the Centre National de la Recherche Scientifique (Paris) and the Direction Générale à la Recherche Scientifique et Technique (Tunis) for constant financial support.

REFERENCES

[1] G. Leibfried and H. D. Z. Dietze, Z. Phys. 126 290 (1949).
[2] F. Kroupa, Czechosl. Jour. Phys. 9 458 (1959).
[3] M. S. Lee and J. Dundurs, Int. J. Engng. Sci. **11** 87 (1973).
[4] R. Bonnet, *C. R. Acad. Sci. Paris* t. **318** 289 (1994).
[5] R. Bonnet, *C. R. Physics* **4** 961 (2003).
[6] B. D. Cullity, *Elements of X-ray diffraction* (Addison-Wesley Pub. Cy., 3d ed. 1967), p. 484.
[7] D. J. H. Cockayne, I. L. F. Ray and Whelan, M. J., *Phil. Mag*. **20** 1265 (1969).
[8] I. L. F. Ray and D. J. H. Cockayne, *Phil. Mag*. **22** 853 (1970) ; *Proc. R. Soc*. A **325** 543 (1971).
[9] A. M. Gomez and D. J. H. Cockayne, P. B. Hirsch, *Phil. Mag*. **31** 105 (1975).
[10] A. M. Gomez and P. B. Hirsch, *Phil. Mag*. **36** 169 (1977).
[11] K. Wessel, and H. Alexander, *Phil. Mag*. **35** 1523 (1977).
[12] G. Packeiser and P. Haasen, *Phil. Mag*. **35** 821 (1977).
[13] H. Föll and D. Ast, *Phil. Mag*. A **40** 589 (1979).
[14] H. Föll, and C. B. Carter, *Phil. Mag*. A **40** 497 (1979).
[15] J. Thibault-Desseaux, H. O. K. Kirchner and J. L. Putaux, *Phil. Mag*. A **60** 385 (1989).
[16] K. Suzuki, N. Maeda, S. and Takeuchi, *Phil. Mag*. A **73** (1996).
[17] K. Rousseau, J.-L. Rouvière, F. Fournel and H. Moriceau, *Appl. Phys. Lett*. **80** 4121 (2002).
[18] A. Reznicek, R. Scholz, S. Senz and U. Gösele, *Mat. Chem. and Phys*. **81** 277 (2003).
[19] M. S. Duesbery and B. Joos, *Phil. Mag*. A **74** 253 (1996).
[20] W. Cai, W., V. V. Bulatov, J. F. Justo, A. S. Argon and S. Yip, *Phys. Rev. Lett*. **84** 3346 (2000).
[21] L. Pizzagalli, P. Beauchamp and J. Rabier, *Phil. Mag*. 83 1191 (2003).
[22] J. Rabier, M. F. Denanot, J. L. Demenet and P. Cordier, *Mat. Sc. And Eng*. A **387-389** 124 (2004).
[23] J. P. Hirth, and J. Lothe, *Theory of dislocations* (2d ed., John Wiley and Sons, New York 1982), p. 837.
[24] A. Y. Belov, R. Scholz and K. Scheerschmidt, *Phil. Mag. Lett*. **79** 531 (1999).
[25] A. Boussaïd, F. Fournel and R. Bonnet, *Phys. Stat. Sol. (a)* 242 3091 (2005).
[26] P. M. Hazzledine, H. P. Karnthaler and E. Wintner, *The Phil. Mag*. **32** 81 (1975).
[27] C. B. Carter, *Phys. Stat. Sol. (a)* **54** 395 (1979).
[28] D. B. Williams and C. B. Carter, *Transmission electron microscopy. Imaging III* (Plenum Press, New York, 1996), p. 434 .
[29] A. Korner, P. Svoboda and H. O. K. Kirchner, *Phys. Stat. Sol. (b)* 441 (1977).
[30] C. H. Belgacem, A. Ati and R. Bonnet, *Phys. Stat. Sol. (b)* 242 R24 (2005).

Corresponding author. Email : rbonnet@ltpcm.inpg.fr

[31] R. Bonnet, *Phil. Mag.* A **43** 1165 (1981).
[32] V. Volterra, *Sur l'équilibre des corps élastiques multiplement connexes,* Archives of the journal *« Annales scientifiques de l'Ecole Normale Supérieure »* (Gauthier-Villars, Editions scientifiques and médicales Elsevier, 1907) 3d series, t. **24** 401.
[33] S. Wolfram, *Mathematica,* software (Wolfram media/Cambridge University Press,1999).
[34] N. Fribourg-Blanc, M. Dupeux, G. Guénin and R. Bonnet *J. Appl. Cryst*. **12** 151 (1979).
[35] A. K. Head, *Proc. of the Phys. Soc*. **B 66** 793 (1953).
[36] M. Dynna, J. L. Vassent, A. Marty and B. Gilles, *J. Appl. Phys*. **80** 2650 (1996).
[37] R. Bonnet, in *Fundamentals of Diffusion Bonding*, Proc. of the First Seiken Int. Symp. On Interface Structure, Properties and Diffusion Bonding (ed. By Y. Ishida, Elsevier Pub., Amsterdam 1987), p.329.
[38] D. J. H. Cockayne, M. L. Jenkins and I. L. F. Ray, *Phil. Mag*. **24** 1383 (1971).

Appendix 1

Some cited papers contain misprints. They are listen as follows :

Réf. [3] : in expression (10a) the term (κ_2-1) should be 2(κ_2-1). In expression (12c) replace the term $2(^2 - t^2)$ by $2(q^2 - t^2)$.

Réf. [4] : in expressions (5) and (7) replace (1+k) by (-1+k). In the second line of expression (8) replace the factor +k by -k. In expression (14) replace $+2h^- n\omega$ by $-2h^- n\omega$. In expression (16) replace the factor k by -k. In the fourth line of expression (20) replace $+(1+2hn\omega)$ by $_x(1+2\ h^+ n\omega)$.

Réf. [31] : in expressions (15) the signs before the two monomials in B_2 shoud be minus. In expression (16) the second monomial in B_3 should be the same monomial but in B_2. In expression (20a), the sign before the second monomial in B_2 should be negative. In the system of linear equations (26), line 12, the second monomial in B_3 should be the same monomial but in B_1. In expression (32c) and function F_6, the first term of the denominator should be written with a positive exponent ($+2\pi$ g $|x_2|$).

Réf. [35]: in p. 797, the numerator of the third fraction giving τ_{xx} should be written without any curly brackets.

Réf. [37]: in p. 333, equation (9), the denominator of the last fraction should include a bar above the variable Z_β^+ (to form the complex conjugate of Z_β^+).

Corresponding author. Email : rbonnet@ltpcm.inpg.fr

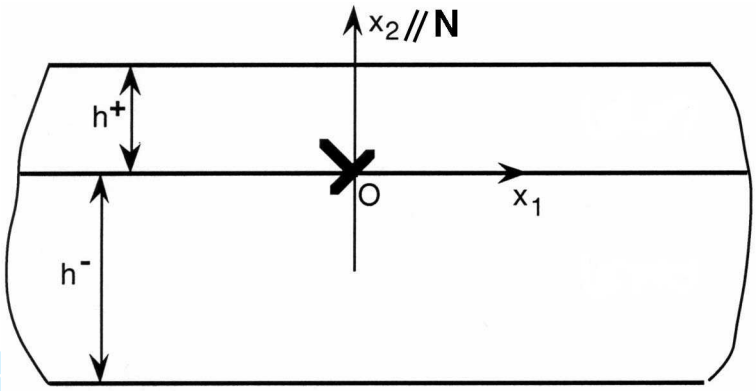

Fig. 1

Thin bicrystalline plate formed by two crystals + and - with thicknesses h^- and h^+. The interface Ox_1Ox_3 contains an array of periodic misfit dislocations parallel to Ox_3. When the period Λ tends to infinity the elastic field around Ox_3 tends to that of a translation dislocation (reverse symbol **T**).

Corresponding author. Email : rbonnet@ltpcm.inpg.fr

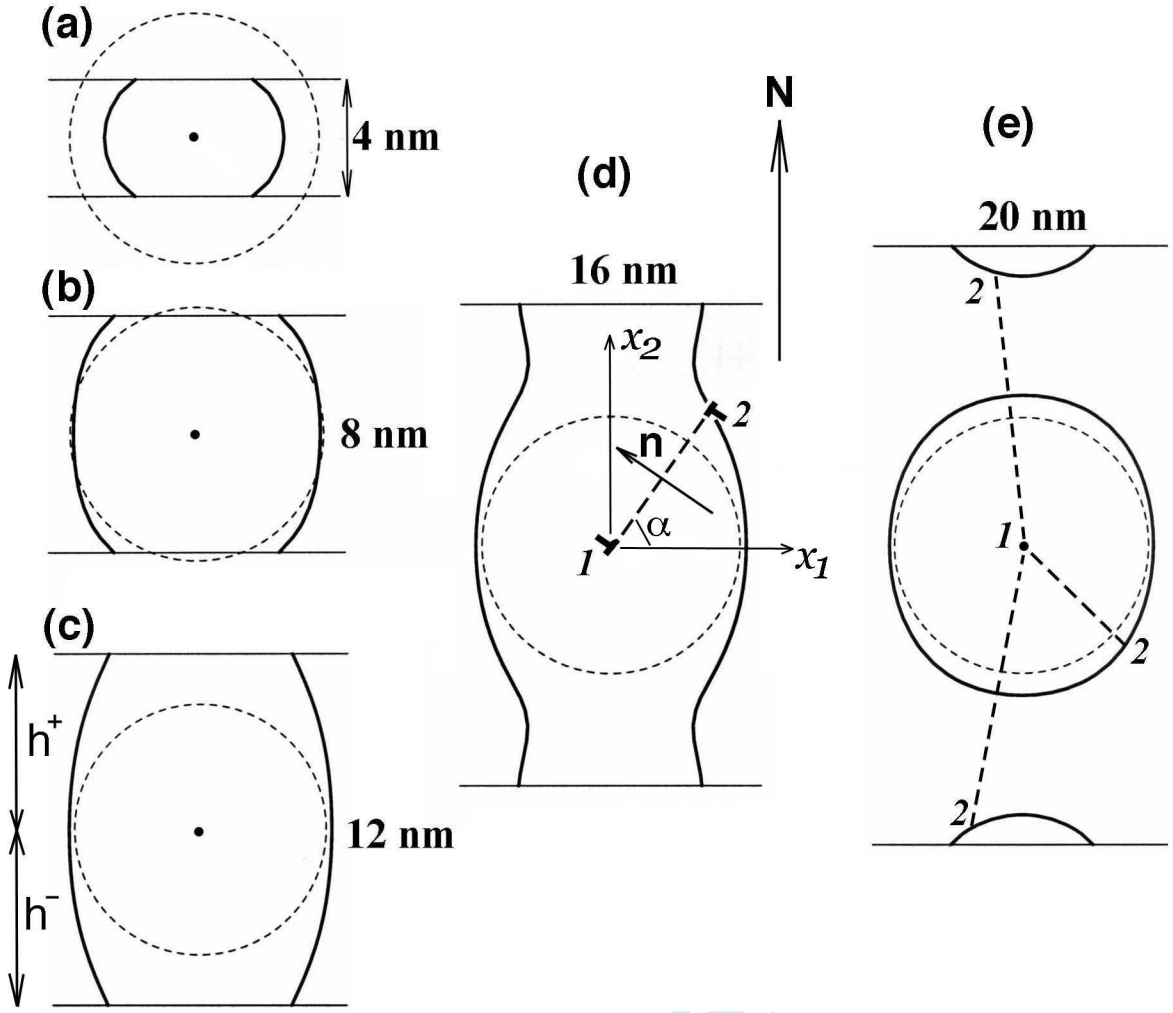

Fig. 2

Dissociation of a [011] screw dislocation located in an isotropic silicon plate. Different possible loci (plain curves) of partial 2 when the $(1\,\bar{1}\,1)$ fault plane (normal **n**) takes different orientations around the fixed partial 1. The normal is **N** and the thickness is $(h^+ + h^-) =$ 4 to 20 nm from (a) to (e)). The locus of partial 2 for an unlimited silicon crystal is a circle (in dotted line).

Corresponding author. Email : rbonnet@ltpcm.inpg.fr

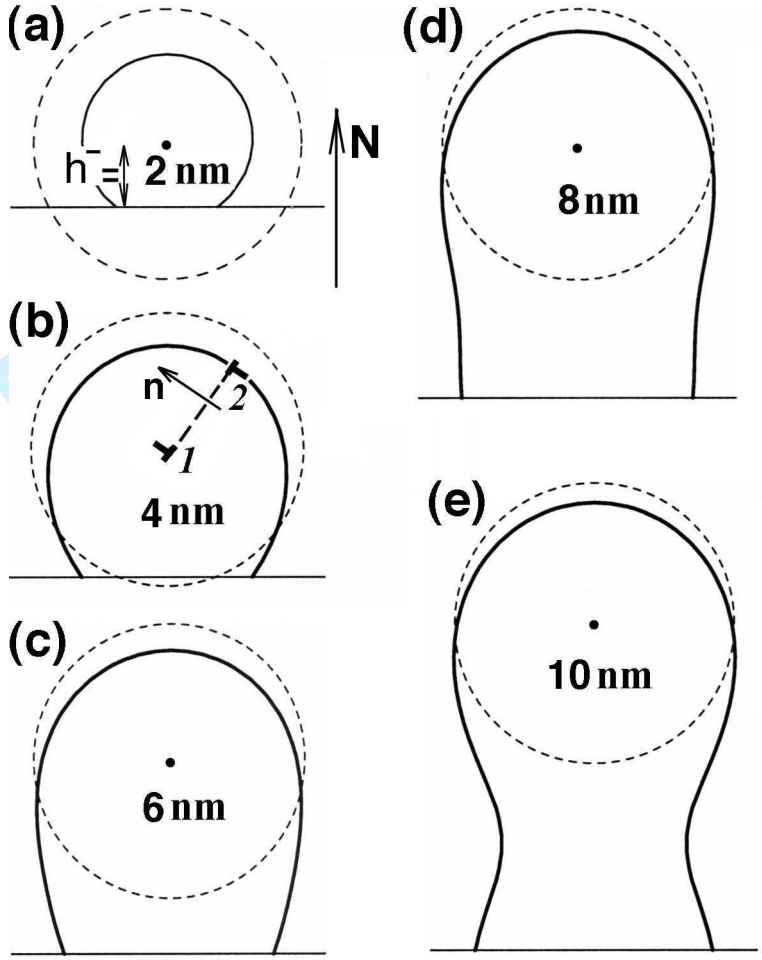

Fig. 3

Possible dissociation schemes of a [011] screw dislocation located in a bottom-limited semi-infinite silicon crystal (isotropic elasticity). The separation distance S between the two Shockley partials 1 and 2 depends on the fault plane orientation **n** and on the position of partial 1 ($h^- = 2$ to 10 nm). The successive distances h^- are the same in graphs (a-e) of figures 2 and 3.

Corresponding author. Email : rbonnet@ltpcm.inpg.fr

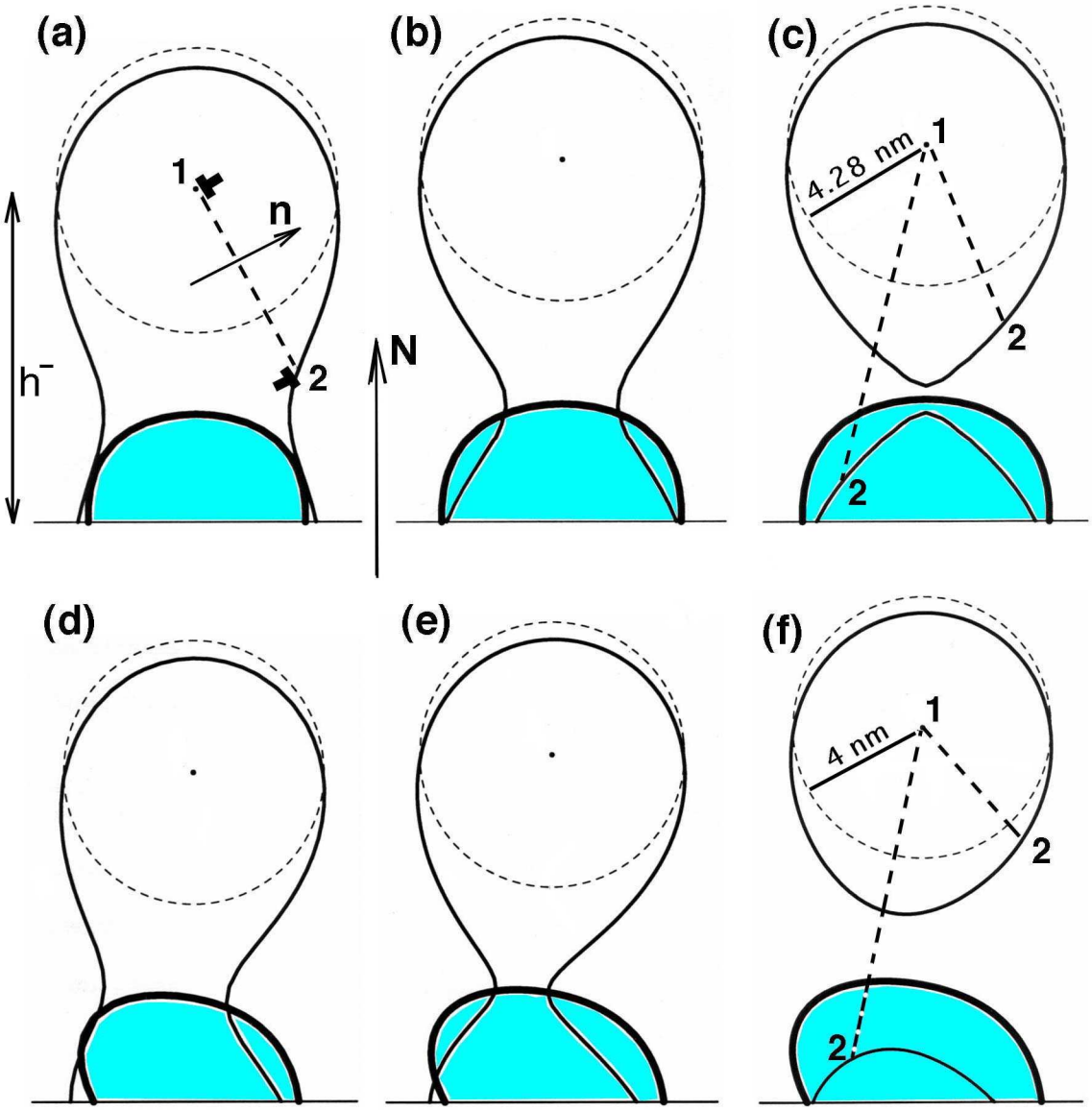

Fig. 4

Possible dissociation configurations of a [011] screw dislocation nearby a bottom-limited semi-infinite silicon crystal in (a-c) isotropic elasticity (h^-= 10, 11, 11.5 nm) and (d-f) anisotropic elasticity (h^-= 10, 10.5, 11.5 nm). Except for graph (a), for which the polar radius cuts only once the locus of partial 2 (plain curve), other graphs exhibits possible unstable equilibriums if the locus of partial 2 is included inside a shaded part of the graph.

Corresponding author. Email : rbonnet@ltpcm.inpg.fr